Turkish Journal of Electrical Engineering & Computer Sciences

http://journals.tubitak.gov.tr/elektrik/

Research Article

Turk J Elec Eng & Comp Sci
(2018) 26: 2406 – 2416

doi:10.3906/elk-1802-19

Method of singular integral equations in diffraction by semiinfinite grating: *E*-polarization case

Mstislav KALIBERDA[1,*], **Leonid LYTVYNENKO**[2], **Sergey POGARSKY**[1]
[1]Department of Radiophysics, V. Karazin National University of Kharkiv, Kharkiv, Ukraine
[2]Institute of Radio Astronomy of the National Academy of Sciences of Ukraine, Kharkiv, Ukraine

Received: 02.02.2018 • **Accepted/Published Online:** 09.05.2018 • **Final Version:** 28.09.2018

Abstract: Diffraction of the *E*-polarized electromagnetic wave by a semiinfinite strip grating is considered. The scattered field is represented as a superposition of the field induced by the currents on the strips of an infinite periodic grating and the field induced by the correction current excited due to end of the grating. A singular integral equation with additional conditions for correction current density is obtained. A solution for the infinite periodic grating in the *E*-polarization case is obtained from the corresponding solution for the *H*-polarization case using the duality principle. Numerical results for the current density and far fields distribution are represented.

Key words: Semiinfinite grating, singular integral equation, diffraction

1. Introduction

In an earlier paper [1], the problem of H-polarized wave diffraction by semiinfinite grating (SIG) was investigated. For full analysis it is necessary to consider the E-polarization case.

Strip gratings may be used as frequency-selective surfaces, components of optic devices, metamaterials, and stealth covers. The model of SIG may be used to study effects caused by truncation of a real finite grating [2–4]. The real gratings may have defects such as break of periodicity or even the absence of one or several strips. The model of the SIG can allow us to describe the difference of the properties of the ideal periodic grating and the real one. However, here researchers may meet some difficulties. The infinite size of SIG does not allow us to directly apply methods of analysis of finite gratings. Despite the fact that SIG is infinite, it cannot be treated as ideally periodic. For this reason the Floquet theorem also is not applied here directly. As a rule, SIGs are studied with the use of the following approach. The total field is sought as the field of the infinite-periodic grating (IPG) and correction field. Often these fields are presented using potentials with unknown current densities on the strips. The vast majority of papers deal with the E-polarization case. Partially it is connected with that integrand that has logarithmic singularity, unlike the H-polarization case. Such integrals are integrable ones. Different approaches may be used to obtain the correction field and scattered field of a whole structure. In [5, 6] the variational approach and in [2, 3, 7] the method of moments (MoM) was proposed. In [8–13], the Wiener–Hopf technique was used, while in [14] the canonical problem was solved by the Sommerfeld–Maliuzhinets method. The operator method [15–19] allows us to study different semiinfinite arrays of scatterers. As a result, a nonlinear operator equation may be obtained. However, as we know, there are some problems with the convergence of the solution schemes of nonlinear equations. In [20], the authors stated

*Correspondence: KaliberdaME@yandex.ua

that direct discretization of integral equations with a logarithmic singularity is not sufficiently effective. The authors managed to obtain more efficient schemes based on the Cauchy-type singular integral equations with their discretization by the method of discrete singularities (MDS). The MDS belongs to the group of so-called Nystrom-type algorithms [20–27]. In the case of SIG, the algorithm described in [1] with a slight modification can be used. It is also based on the MDS. Such an algorithm uses direct discretization of the singular integral equations. The interpolation procedure involves the Gauss–Chebyshev quadrature formulas. These formulas describe the edge behavior of the fields correctly. Well-known theorems [25, 26] guarantee the convergence of the MDS.

2. Solution of the problem

Let us consider scattering of the E-polarized plane wave by the SIG. The corresponding geometry and the problem notations are shown in Figure 1. The strips have zero thickness and width $2d$, and the period is l. The set of strips we denote as $L = \bigcup_{m=0}^{\infty} (-d + lm;\, d + lm)$. Suppose that the plane wave is incident on the grating from the $z > 0$ half space

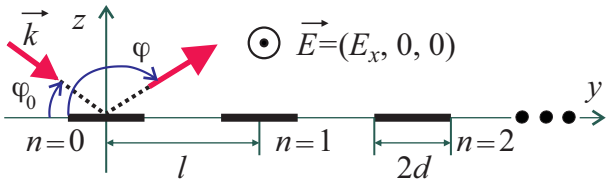

Figure 1. Structure geometry.

$$E_x^i(y,z) = \exp\left(ik(y\cos\varphi_0 - z\sin\varphi_0)\right),$$

where k is the wavenumber and φ_0 is the incident angle to the y-axis. As in the H-polarization case, we seek the scattered field as a sum of two fields. One of them is the field of currents on the IPG and the other one is the correction field,

$$E_x^s(y,z) = E_x^{s,inf}(y,z) + E_x^{s,c}(y,z). \tag{1}$$

The field of currents on IPG $E_x^{s,inf}(y,z)$ we represent in the form of single-layer potential [28]. Correction field $E_x^{s,c}(y,z)$ also can be represented as single-layer potential (for example, as in [2, 3]), but here we represent $E_x^{s,c}(y,z)$ in the spectral domain via an unknown spectral function,

$$E_x^{s,inf}(y,z) = \frac{i\omega\mu_0}{4}\sum_{m=0}^{\infty}\int_{-d}^{d}\mu_m^{\infty}(y'+lm)H_0^{(1)}\left(k\sqrt{(y-y'-lm)^2+z^2}\right)dy', \tag{2}$$

$$E_x^{s,c}(y,z) = \int_{-\infty}^{\infty} c(\xi)\exp\left(ik(\xi y + \gamma(\xi)|z|)\right)d\xi, \tag{3}$$

where $\mu_m^{\infty}(y'+lm)$ is equal up to a factor to the current density on the mth strip of the IPG, $c(\xi)$ is an unknown spectral function of the correction field, $\gamma(\xi) = \sqrt{1-\xi^2}$, $Re\gamma \geq 0$, $Im\gamma \geq 0$, $H_0^{(1)}(x)$ is the Hankel

function of the first kind, μ_0 is a magnetic constant, and ω is angular frequency. The summation is performed over all strips of the SIG, $m = 0, 1, 2, ...$

Enforcement of boundary conditions leads to the dual integral equations:

$$\int_{-\infty}^{\infty} c(\xi)\gamma(\xi)\exp(ik\xi y)d\xi = 0,\ y \notin L, \tag{4}$$

$$\int_{-\infty}^{\infty} c(\xi)\exp(ik\xi y)d\xi = -\left(E_x^i(y,0) + E_x^{s,inf}(y,0)\right) = g(y),\ y \in L. \tag{5}$$

From Eq. (1) we can obtain an expression for $g(y)$:

$$g(y) = \frac{\omega\mu_0}{2}\sum_{m=-\infty}^{-1}\exp\left(ik\zeta_0 lm\right)\int_{-d}^{d} H_y^{s,inf}(y',0)H_0^{(1)}\left(k\sqrt{(y-y'-lm)^2+z^2}\right)dy',$$

where in the general case $\zeta_m = \frac{2\pi m}{kl} + \cos\varphi_0$. Here we used the Floquet theorem and the expression for $\mu_0^{\infty}(y)$,

$$\mu_0^{\infty}(y) = \begin{cases} \frac{2}{i}H_y^{s,inf}(y,0), & |y| \le d, \\ 0, & |y| > d. \end{cases}$$

From the Maxwell equations it follows that the tangential magnetic component of the field of the IPG is

$$H_y^{s,inf} = \frac{1}{i\omega\mu_0}\frac{\partial E_x^{s,inf}}{\partial z}. \tag{6}$$

2.1. Singular integral equation

From edge conditions, as well as from Eq. (4), it follows that $c(\xi)$ may have singularities when $\xi \to \pm 1$. Let us introduce function $u(\xi) = \gamma(\xi)c(\xi)$, which does not have singularities. Eq. (4) is the Fourier transform of $u(\xi)$ and it is valid for $y \notin L$. Let us consider the Fourier transform of $u(\xi)$ for all $y \in (-\infty; \infty)$ and denote it as $F(y)$:

$$F(y) = \int_{-\infty}^{\infty} u(\xi)\exp(iky\xi)d\xi.$$

Then, using the inverse Fourier transform, we can express function $u(\xi)$ as follows:

$$u(\xi) = \frac{k}{2\pi}\int_{L} F(y)\exp(-iky\xi)dy.$$

Let us differentiate Eq. (5) with respect to y. Then the following singular integral equation can be obtained [20, 25–27]:

$$\frac{1}{\pi}PV\int_{L}\frac{F(\xi)}{\xi - y}d\xi + \frac{1}{\pi}\int_{L}K(y,\xi)F(\xi)d\xi = \frac{i}{k}g'(y),\ y \in L, \tag{7}$$

where PV means the Cauchy principal value integral. Eq. (4) gives rise to additional conditions:

$$\frac{1}{\pi}\int\limits_{L} F(\xi)Q(y_m,\xi)d\xi = g(y_m),\ m=0,\ 1,\ ..., \tag{8}$$

where y_m is an arbitrary point of $(-d+lm;\ d+lm)$. The kernel functions are

$$K(y,\xi) = k\int\limits_{0}^{\infty}\frac{\sin(k\zeta(y-\xi))}{\zeta}(\zeta+i\gamma(\zeta))d\zeta,$$

$$Q(y,\xi) = k\int\limits_{0}^{\infty}\frac{\cos(k\zeta(y-\xi))}{\gamma(\zeta)}d\zeta.$$

The solution of Eqs. (7) and (8) can be obtained by the MDS [20, 25, 26]. Note that the right-hand sides of Eqs. (7) and (8), $g(y)$ and $g'(y)$, are still unknown. To evaluate them we should consider the IPG and obtain an expression for $H_y^{s,inf}(y,0)$.

2.2. Field $H_y^{s,inf}(y,z)$

To obtain the field scattered by the IPG in the E-polarization case we use the duality principle and the known solution for the H-polarization case. For the scattered field written as a Fourier series with unknown amplitudes $a_n,\ n=-\infty,...+\infty$,

$$E_x^{s,inf}(y,z) = \sum_{n=-\infty}^{\infty} a_n \exp\left(ik(\zeta_n y+\gamma_n|z|)\right), \tag{9}$$

where $\gamma_n = \sqrt{1-\left(\frac{2\pi n}{kl}+\cos\varphi_0\right)^2}$, $Re\gamma_n \geq 0$, $Im\gamma_n \geq 0$, and the singular integral equation similar to Eq. (7) with an additional condition can be obtained [25–27]:

$$\frac{1}{\pi}PV\int\limits_{S}\frac{F_{2\pi}(\xi)}{\xi-\psi}d\xi + \frac{1}{\pi}\int\limits_{S}K_{2\pi}(\psi,\xi)F_{2\pi}(\xi)d\xi = i\kappa\gamma_0,\ \psi\in slot, \tag{10}$$

$$\frac{1}{\pi}\int\limits_{S}F_{2\pi}(\xi)d\xi = 0. \tag{11}$$

The kernel function is

$$K_{2\pi}(\psi,\xi) = -\frac{\kappa}{2}\sum_{\substack{n=-\infty\\ n\neq 0}}^{\infty}\left(\frac{i|n|}{\kappa}-\gamma_n\right)\frac{\exp\left(in(\psi-\xi)\right)}{n} + i\gamma_0\kappa\frac{\psi-\xi}{2} + \left(\frac{1}{\psi-\xi}-\frac{1}{2}ctg\left(\frac{\psi-\xi}{2}\right)\right),$$

where $\kappa = kl/(2\pi)$ is a dimensionless wave number. Integration is performed over slot S of a single period (in dimensionless quantities). The singular integral equation with additional conditions, Eqs. (10) and (11),

also can be solved by the MDS. Amplitudes a_n can be expressed via $F_{2\pi}$ with the help of the periodic Fourier transform:

$$a_n = \frac{\exp(-i\pi n)}{2\pi i n} \int\limits_S F_{2\pi}(\xi) \exp(-in\xi) d\xi, \ n \neq 0,$$

$$a_0 = -\frac{1}{\pi} \int\limits_S \frac{\xi}{2} F_{2\pi}(\xi) d\xi - 1.$$

Eq. (9) is obtained from the condition that current density outside the metal strips be 0. For the metal strips one can obtain the following:

$$H_y^{s,inf}(y,0) = \frac{\exp(iky\sin\alpha)}{i\kappa Z} \left(\frac{1}{\pi} v.p. \int\limits_{-\delta}^{\delta} \frac{F(\xi)}{\xi - \psi} d\xi + \frac{1}{\pi} \int\limits_{-\delta}^{\delta} K(\psi,\xi) F(\xi) d\xi - i\kappa\gamma_0 \right), \tag{12}$$

where Z is free space impedance.

3. Field representation

3.1. Far field

To express far fields we use the saddle-point method [29]. However, here one should use a higher-order asymptotic than in the case of regular finite grating. The semiinfinite summation in Eq. (2), $m = 0, 1, 2, \ldots$, leads to the poles' appearance in the integrands. The position of poles corresponds to the cut-off frequencies of the plane waves, which exist only in the domain $\varphi > w_q$, where w_q is the propagation angle of the qth plane wave relative to the y-axis. Line $\varphi = w_q$ acts as a shadow boundary [1–3, 18]. Then

$$E_x^s(\varphi,\rho) \cong E_x^p(\varphi,\rho) + E_x^{erfc}(\varphi,\rho) + E_x^{s,c}(\varphi,\rho), \ k\rho \to \infty, \tag{13}$$

where $\rho = \sqrt{y^2 + z^2}$ is distance. By substituting Eq. (9) into Eq. (6) and then into Eq. (2), and using Eqs. (1) and (3), we may rewrite terms in Eq. (13) in explicit form:

$$E_x^p(\varphi,\rho) = \sum_q \varepsilon_q(\varphi) a_q \exp(ik\rho\cos(\varphi - w_q)). \tag{14}$$

The following function appears:

$$\varepsilon_q(\varphi) = \begin{cases} 0, & \varphi < w_q, \\ 1, & \varphi > w_q, \end{cases}$$

since, as was mentioned above, plane waves exists only in the $\varphi > w_q$ domain. The second-order asymptotic gives us the Gauss error function in $E_x^{erfc}(\varphi,\rho)$. It provides continuous asymptotic representation in the

transition region near $\varphi = w_q$,

$$E_x^{erfc}(\varphi,\rho) = \exp\left(ik\rho - \tfrac{\pi i}{4}\right)\left[\tfrac{\pi}{kl}\sum_q sgn(w_q-\varphi)\tfrac{c^{inf}(-\cos w_q)}{\sin w_q}\times\right.$$
$$\left.\exp\left(-2ik\rho\left(\sin\tfrac{\varphi-w_q}{2}\right)^2\right)\cdot\left(\tfrac{1+i}{\sqrt{2}} - \sqrt{2}C(\psi) - \sqrt{2}iS(\psi)\right) - \tfrac{i}{kl}\sqrt{\tfrac{\pi}{2k\rho}}\left(\tfrac{2c^{inf}(-\cos\varphi)}{f(-\cos\varphi)} + \sum_q \tfrac{c^{inf}(-\cos w_q)}{\sin w_q \sin\frac{w_q-\varphi}{2}}\right)\right], \tag{15}$$

where

$$C(\psi) = \int_0^{\psi}\cos\left(\frac{\pi}{2}t^2\right)dt,$$

$$S(\psi) = \int_0^{\psi}\sin\left(\frac{\pi}{2}t^2\right)dt,$$

are Fresnel integrals, $\psi = 2\sqrt{\frac{k\rho}{\pi}}\sin\left|\frac{w_l-\varphi}{2}\right|$, $w_q = \pi/2 + \arcsin\zeta_q$, $f(\xi) = 1 - \exp\left(ikl(\cos\varphi_0 - \xi)\right)$, $c^{inf}(\xi) = 2\sum\limits_{n=-\infty}^{\infty} a_n\gamma_n\frac{\sin(kd(\zeta_n-\xi))}{kl(\zeta_n-\xi)}$, and $\sum\limits_q$ is the summation over all q that correspond to the propagating plane waves, $|\zeta_q| < 1$. Notice that here we used Eq. (9) but not Eq. (12). This was done to obtain Eq. (14) in a simple form as a sum of propagating Floquet modes.

The far field for Eq. (4) is

$$E_x^{s,c}(\varphi,\rho) \cong \sqrt{\frac{2\pi}{k\rho}}u(-\cos\varphi)\exp\left(i(k\rho - \pi/4)\right),\ 0 < \varphi < \pi.$$

3.2. Current on the strips

Function $F(y)$ in Eqs. (7) and (8) equals up to a constant factor $(2/Z)$ to a correction current density on the strips. Thus, to evaluate correction current density, we may use $F(y)$. According to the edge condition, current density has root-type singularity near the edge. To describe the correction current behavior we introduce function

$$J_c(y) = \sqrt{(y-(-d+lm))\left((d+lm)-y\right)}F(y),$$

$$y \in (-d+lm;\ d+lm),\ m = 0,\ 1,\ 2,\ ...,$$

which does not have singularities.

4. Numerical results

4.1. Validation and convergence

To validate the obtained results we will compare them with those obtained by the MoM in the assumption of a single-mode current distribution [2]. For better visual comparison with results obtained in [2], we introduce

coefficient J_n^c, which is up to a constant factor the correction current density in the center of the nth strip when $y = y_n = l \cdot n$,

$$J_n^c = \frac{d}{Z\pi} J_c(y_n).$$

The diffraction pattern without Floquet modes we denote as

$$D(\varphi, \rho) = E_x^{erfc}(\varphi, \rho) + E_x^{s,c}(\varphi, \rho).$$

The results for J_n^c are represented in Figure 2 and diffraction patterns are represented in Figure 3. Good agreement is observed between our results and results obtained by the MoM. Far from the shadow boundaries ($\varphi = w_q$) the behavior of $D(\varphi, \rho)$ is mainly defined by the field of cylindrical waves. Its magnitude vanishes as $E_x^{sc}(\varphi, \rho) \sim 1/\sqrt{k\rho}$, when $k\rho \to \infty$. However, near the shadow boundaries $E_x^{erfc}(\varphi, \rho)$ dominates. As one can see from Figure 3, $D(\varphi, \rho)$ does not vanish near $\varphi = w_q$.

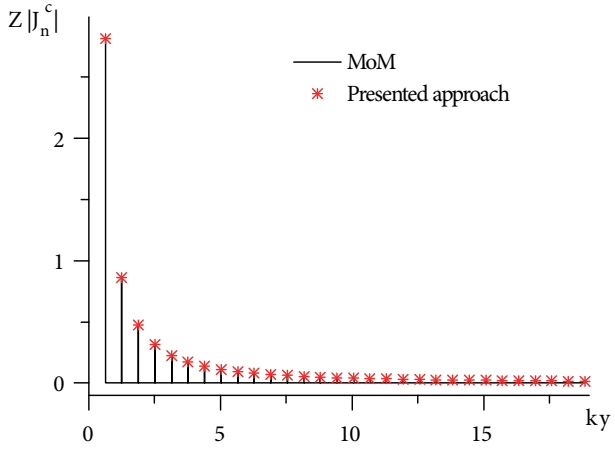

Figure 2. Distribution of $|J_n^c|$ vs. y, $kl = \pi/5$ ($l = \lambda/10$), $kd = \pi/20$ ($2d = \lambda/20$), $\varphi_0 = 90^0$. Presented approach (asterisks) and method from [2] (solid line).

To solve Eqs. (7), (8), (10), and (11) we use the quadrature rule for singular integrals with root-type weight function [20, 25, 26]. Denote the number of nodes on every strip as M. We suppose that the edge of the SIG is influenced at the finite number of strips N. We exchange the infinite set of strips L by the bounded one $L_N = \bigcup_{m=0}^{N} (-d + lm;\, d + lm)$. Let us quantify the correction current influence by the following value [1–3]:

$$J^c = \int_L |J_c(y)|^2 \, dy.$$

Figure 4a shows the relative error of correction current $\varepsilon_M = |(J^c(M) - J^c(2M))/J^c(2M)|$ versus M, and Figure 4b shows the relative error of correction current $\varepsilon_N = |(J^c(N) - J^c(2N))/J^c(2N)|$ versus N. Notice that convergence is provided by general theorems [25, 26]. The value of parameter $kd = \pi/2$ corresponds to the resonance region and strip width is equal to half of the wavelength, $2d = \lambda/2$. The value of parameter $kl = 2\pi$ ($l = \lambda$) corresponds to the cut-off frequency of ± 1 Floquet modes. It is obvious that the larger the strip width

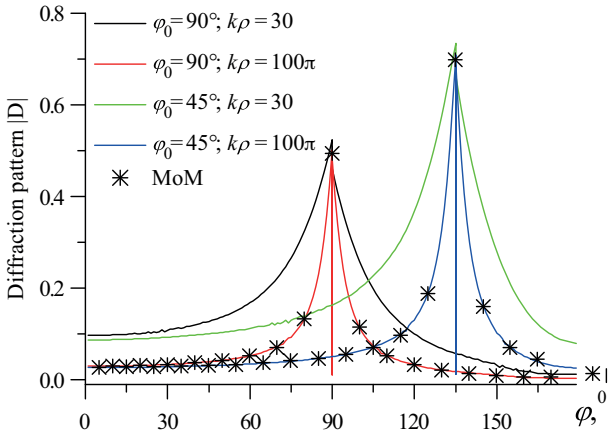

Figure 3. Diffraction patterns, $kl = \pi/5$ ($l = \lambda/10$), $kd = \pi/20$ ($2d = \lambda/20$) for two different incident angles, $\varphi_0 = 90^0$ and $\varphi_0 = 45^0$, and two different distances from the grating to the observation point, $k\rho = 30$ and $k\rho = 100\pi$. Presented approach (solid lines) and method from [2] (asterisks).

is, the larger number of interpolation nodes should be taken. The biggest error of ε_N as expected is observed near the cut-off frequency of the Floquet modes.

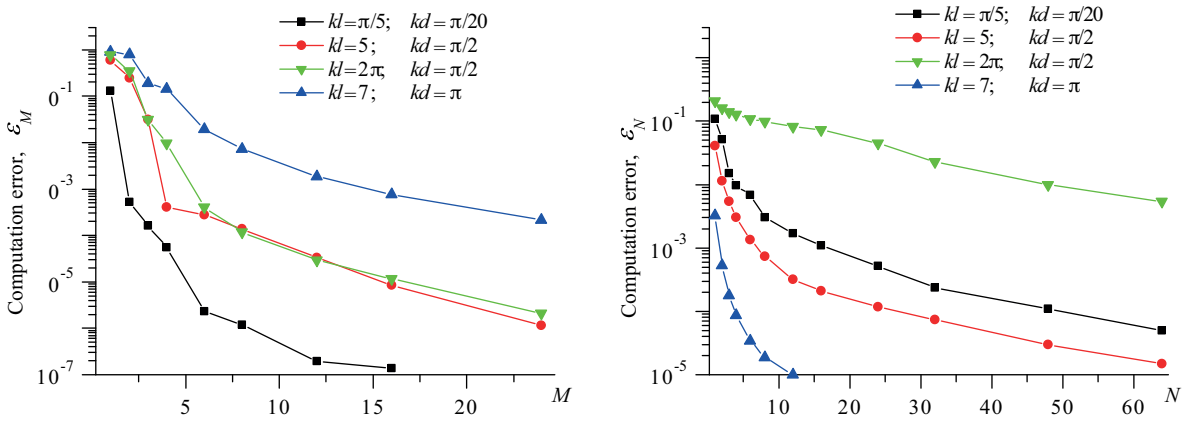

Figure 4. Computation error. a) ε_M as a function of number of nodes on every strip; b) ε_N as a function of number of strips.

4.2. Numerical analysis

Figures 5a, 5b, 5c, and 5d show diffraction patterns of the correction and total current at distance $k\rho = 100\pi$ ($\rho = 50\lambda$) for different values of period and strip width. For comparison, the Kirchhoff solution ($E_x^{s,c}(\varphi, \rho) \equiv 0$) is also shown in Figure 5. The plots are normalized by the maximum value for $kd = \pi/2$, $kl = 2\pi$. The maxima in patterns are observed near the angles of propagation of the Floquet modes. The curves for $D(\varphi, \rho)$ may have discontinuities here [1–3]. However the total scattered field is continuous since term $E_x^p(\varphi, \rho)$ should be added. A jump discontinuity at $\varphi = w_q$ appears because of term $sgn(w_q - \varphi)$ in Eq. (15), and $E_x^s(\varphi \to w_q - 0, \rho) - E_x^s(\varphi \to w_q + 0, \rho) = E_x^p(\varphi \to w_q + 0, \rho)$. At the finite strip gratings in the E-polarization case the leaky waves propagating near $\varphi = 0^0$ and $\varphi = 90^0$ excite not only near $l = n \cdot \lambda$, $n = 1, 2, \ldots$ but at all

frequencies. Case $l = n \cdot \lambda$, $n = 1, 2, ...$ corresponds to the Wood anomaly region when high-order propagating Floquet modes arise. Figure 5b is plotted for the first Wood anomaly, $l = \lambda$. Moreover, the resonant width of the strips is taken, $2d = \lambda/2$. One may observe significant increase in the intensity of the correction field near the plane of the grating. Here leaky waves lead to the appearance of additional maxima near the plane of the SIG.

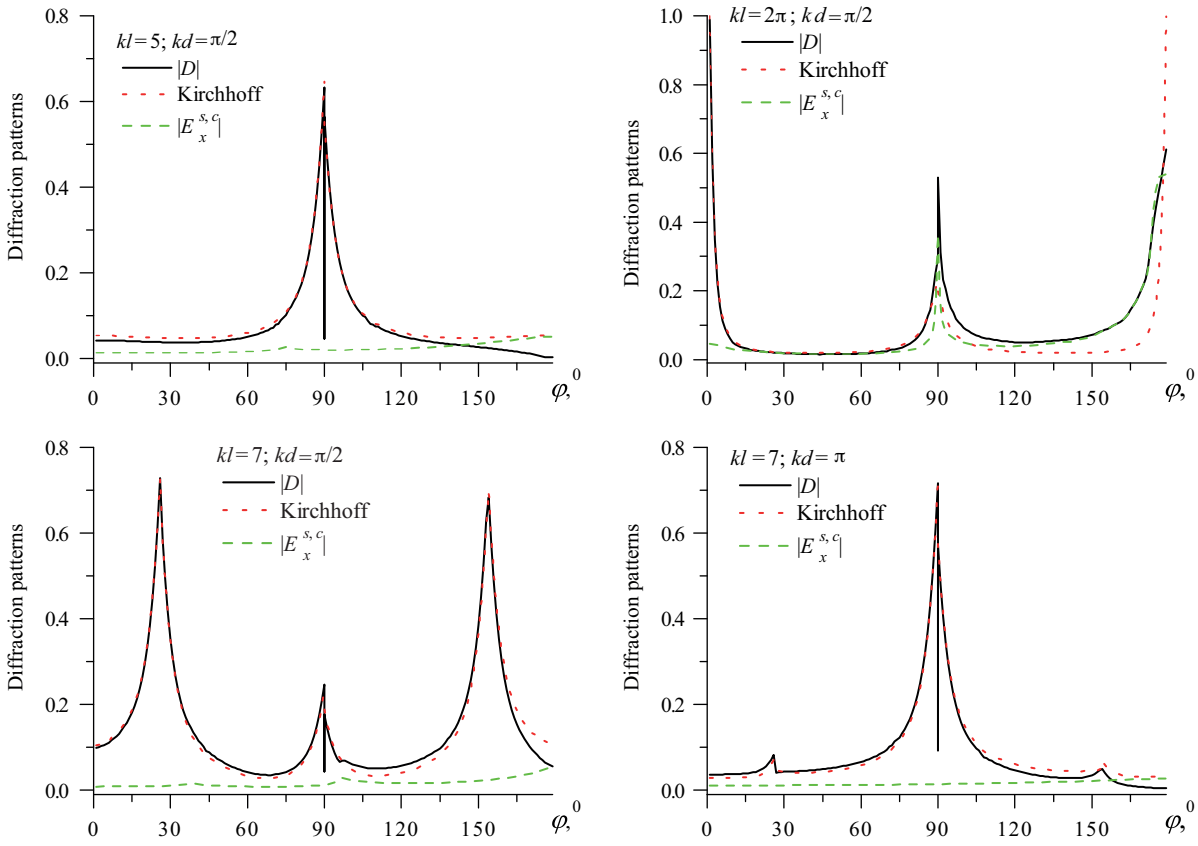

Figure 5. Diffraction patterns, $k\rho = 100\pi$ ($\rho = 50\lambda$). Function $|D(\rho, \varphi)|$ (black solid lines), Kirchhoff solution (red dotted lines), and correction field (green dashed lines): a) $kl = 5$, $kd = \pi/2$ ($2d = \lambda/2$); b) Wood anomaly $kl = 2\pi$ ($l = \lambda$), $kd = \pi/2$ ($2d = \lambda/2$); c) $kl = 7$, $kd = \pi/2$ ($2d = \lambda/2$); d) $kl = 7$, $kd = \pi$ ($2d = \lambda$).

It is known [24, 27, 30] that in the E-polarization case, contrary to the H-polarization case, when parameters of the grating close to the exciting of the Wood anomaly are chosen, the strips' interaction in the regular IPG is weak. The reflection coefficient of the IPG is much smaller as compared to the H-polarization case. The same situation was described in [24, 27] when a single strip was removed from the IPG. Another picture is observed in the case of the SIG. Diffraction patterns presented in Figure 5 show that there is significant disturbance in the scattered field near the Wood anomaly region. Figure 6 and Figure 7 allow us to make a conclusion about the influence of the end of the SIG. These figures show the correction current distribution on the strips and dependence of J^c versus period l. The correction current vanishes away from the SIG edge, as we expected. The maxima of J^c appear near the Wood anomaly regions. The same situation was observed in the H-polarization case, too [1].

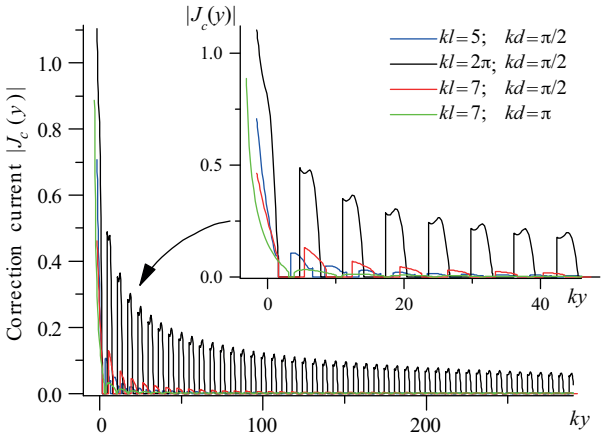

Figure 6. Distribution of $|J_c(y)|$ vs. y, $kl = 5$, $kd = \pi/2$ (blue line), Wood anomaly $kl = 2\pi$, $kd = \pi/2$ (black line), $kl = 7$, $kd = \pi/2$ (red line), and $kl = 7$, $kd = \pi$ (green line).

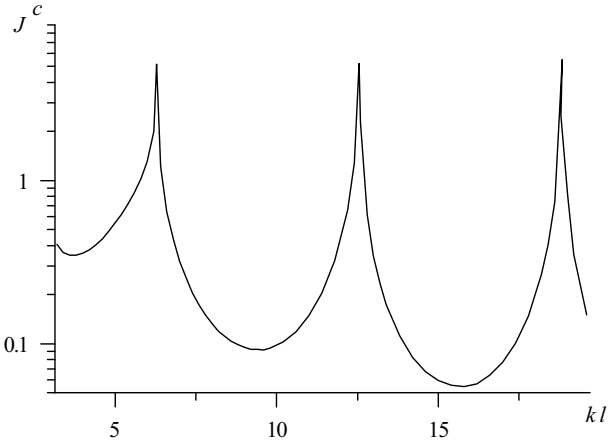

Figure 7. Correction current influence, $kd = \pi/2$.

5. Conclusion

In this paper, a rigorous solution of the E-polarized plane wave diffraction by the SIG is obtained. The total field is presented as a superposition of the field of currents on the IPG and correction field. These fields are obtained as a result of the solution of singular integral equations. The method of numerical solution provides a theoretically guaranteed convergence.

It was shown that there is significant disturbance in the scattered field near the Wood anomaly region when high-order propagating Floquet modes arise. Contrary to the IPG one may observe an increase of the current magnitude on the SIG near this region.

References

[1] Kaliberda M, Lytvynenko L, Pogarsky S. Method of singular integral equations in diffraction by semi-infinite grating: H-polarization case. Turk J Electr Eng & Comp Sci 2017; 25: 4496-4509.

[2] Nishimoto M, Ikuno H. Analysis of electromagnetic wave diffraction by a semi-infinite strip grating and evaluation of end-effects. Prog Electromagn Res 1999; 23: 39-58.

[3] Nishimoto M, Ikuno H. Numerical analysis of plane wave diffraction by a semi-infinite grating. T IEE Japan 2001; 121-A: 905-910.

[4] Cho YH. Arbitrarily polarized plane-wave diffraction from semi-infinite periodic grooves and its application to finite periodic grooves. Prog Electromagn Res M 2011; 18: 43-54.

[5] Fel'd YN. Electromagnetic wave diffraction by semi-infinite grating. J Commun Technol Electron 1958; 3: 882-889.

[6] Fel'd YN. On infinite systems of linear algebraic equations connected with problems on semi-infinite periodic structures. Doklady AN USSR 1955; 114: 257-260 (in Russian with an abstract in English).

[7] Caminita F, Nannetti M, Maci S. An efficient approach to the solution of a semi-infinite strip grating printed on infinite grounded slab excited by a surface wave. In: XXIX URSI General Assembly; 7–13 August 2008; Chicago, IL, USA.

[8] Hills NL, Karp S.N. Semi-infinite diffraction gratings–I. Commun Pur Appl Math 1965; 18: 203-233.

[9] Hills NL. Semi-infinite diffraction gratings–II, inward resonance. Commun Pur Appl Math 1965; 18: 385-395.

[10] Wasylkiwskyj W. Mutual coupling effects in semi-infinite arrays. IEEE T Antenn Propag 1973; 21: 277-285.

[11] Linton CM, Porter R, Thompson I. Scattering by a semi-infinite periodic array and the excitation of surface waves. SIAM J Appl Math 2007; 67: 1233-1258.

[12] Hadad Y, Steinberg BZ. Green's function theory for infinite and semi-infinite particle chains. Phys Rev B 2011; 84: 125402.

[13] Capolino F, Albani M. Truncation effects in a semi-infinite periodic array of thin strips: A discrete Wiener-Hopf formulation. Radio Sci 2009; 44: 1-14.

[14] Nepa P, Manara G, Armogida A. EM scattering from the edge of a semi-infinite planar strip grating using approximate boundary conditions. IEEE T Antenn Propag 2005; 53: 82-90.

[15] Kaliberda ME, Litvinenko LN, Pogarskii SA. Operator method in the analysis of electromagnetic wave diffraction by planar screens. J Commun Technol Electron 2009; 54: 975-981.

[16] Vorobyov SN, Lytvynenko LM. Electromagnetic wave diffraction by semi-infinite strip grating. IEEE T Antenn Propag 2011; 59: 2169-2177.

[17] Lytvynenko LM, Kaliberda ME, Pogarsky SA. Solution of waves transformation problem in axially symmetric structures. Frequenz 2012; 66: 17-25.

[18] Lytvynenko LM, Kaliberda ME, Pogarsky SA. Wave diffraction by semi-infinite venetian blind type grating. IEEE T Antenn Propag 2013; 61: 6120-6127.

[19] Kaliberda ME, Lytvynenko LM, Pogarsky SA. Diffraction of H-polarized electromagnetic waves by a multi-element planar semi-infinite grating. Telecommun Radio Eng 2015; 74: 348-357.

[20] Nosich AA, Gandel YV. Numerical analysis of quasioptical multireflector antennas in 2-D with the method of discrete singularities: E-wave case. IEEE T Antenn Propag 2007; 55: 399-406.

[21] Shapoval OV, Sauleau R, Nosich AI. Scattering and absorption of waves by flat material strips analyzed using generalized boundary conditions and Nystrom-type algorithm. IEEE T Antenn Propag 2011; 59: 3339-3346.

[22] Tsalamengas J. Exponentially converging Nystrom's methods for systems of SIEs with applications to open/closed strip or slot-loaded 2-D structures. IEEE T Antenn Propag 2006; 54: 1549-1558.

[23] Tong MS, Chew WC. Nystrom method with edge condition for electromagnetic scattering by 2-D open structures. Prog Electromagn Res 2006; 62: 49-68.

[24] Kaliberda ME, Lytvtnenko LM, Pogarsky SA. Singular integral equations in diffraction problem by an infinite periodic strip grating with one strip removed. J Electromagnet Wave 2016; 30: 2411-2426.

[25] Gandel YV. Method of discrete singularities in electromagnetic problems. Problems of Cybernetics 1986; 124: 166-183 (in Russian with an abstract in English).

[26] Gandel YV. Boundary-value problems for the Helmholtz equation and their discrete mathematical models. Journal of Math Sciences 2010; 171: 74-88.

[27] Kaliberda ME, Lytvtnenko LM, Pogarsky SA. Singular integral equations in diffraction problem by an infinite periodic strip grating with one strip removed: E–polarization case. J Electromagnet Wave 2018; 32: 332-347.

[28] Luneburg E, Westfahl K. Diffraction of plane waves by an infinite strip grating. Ann Phys 1971; 27: 257-288.

[29] Felsen LB, Marcuvits N. Radiation and Scattering of Waves. Englewood Cliffs, NJ, USA: Prentice Hall, 1973.

[30] Shestopalov VP, Lytvynenko LM, Masalov SA, Sologub VG. Waves Diffraction by the Gratings. Kharkov, Ukraine: Kharkov State University, 1973 (in Russian with an abstract in English).